FxLMS-based Active Noise Control: A Quick Review

Iman Tabatabaei Ardekani, Waleed H. Abdulla
The University of Auckland, Private Bag 92019, Auckland, New Zealand

***Abstract*—This paper represents a short review on active noise control (ANC) with the emphasis on ANC systems implemented by using FxLMS adaptation algorithm. The physical mechanism behind active noise control, based on which local silence zones can be created is detailed. Basic configurations for realization of ANC systems are then introduced. It is shown that FxLMS algorithm has been widely used in different types of ANC systems. Available theoretical work on analysis of FxLMS-based ANC systems is reviewed. Shortcomings of available theoretical findings are discussed. Finally, recent advances in theoretical analysis of FxLMS-based ANC systems are introduced. These advances can be considered as the recent contributions made by the authors. Simulation results are also used to demonstrate the validity of the theoretical findings.**

I. Introduction

Active Noise Control (ANC), in which an electro-acoustic system is responsible to create a local silence zone, has received considerable interest, recently. The first patent on active noise control was granted to a German engineer in 1936 [1]. For two decades this idea remained only a theory on paper until Olson used early analog electronic technology to invent the first ANC device, called the "electronic sound absorber" [2], [3]. By the end of the 1950's, several analog ANC devices were invented, including those invented by Fogel [4], Simshauser [5] and Bose. However, all of analog ANC devices are not able to adapt to changing characteristics of the noise to be canceled and changing environmental conditions. This is because they cannot enjoy any adaptive control technique. Only with the advent of digital technology did the realization of adaptive ANC systems become possible. The theory of adaptive ANC, in which an adaptation algorithm automatically adjusts the ANC device, was established by Widrow in 1975 [6]; however the most significant progresses on this subject was reported in the recent two decades [7], [8].

A. Physical Principles of Active Noise Control

Sound waves are described by variations in the acoustic pressure through space and time. The acoustic pressure is defined as the local deviation from the ambient atmospheric pressure caused by a sound wave. This scalar quantity, which can be directly measured using a microphone in air, is the force (N) of sound on a surface area (m^2) perpendicular to the direction of the sound. The evolution of the acoustic pressure as a function of position and time can be described by the wave propagation equation in three-dimensional space as

$$\nabla^2 p\left(x,y,z,t\right) - \frac{1}{c^2}\frac{\partial^2}{\partial t^2} p\left(x,y,z,t\right) = 0 \tag{1}$$

where $p\left(x,y,z,t\right)$ denotes the acoustic pressure at position (x,y,z) and continuous time t, operator ∇^2 is the Laplacian and constant c is the propagation speed of the sound in the ambient. In [9], it is shown that the propagation of an acoustic wave through the wave propagation process, given in Eq. (1), can be effectively modeled as a linear process.

1) Superposition Property: In system theory, the superposition property states that, for all linear systems, the net response at a given position and time caused by two or more sources is the algebraic sum of the responses, which would have been caused by each source acting individually. Therefore, based on the linearity of the acoustic wave propagation process, the net acoustic pressure at position (x,y,z) and (discrete) time index n caused by two or more sound sources, can be expressed as the algebraic sum of the acoustic pressures, caused by each sound source acting individually. Accordingly, in a general case with N sound sources, the net acoustic pressure at position (x,y,z) and time index n can be expressed as

$$p\left(x,y,z,n\right) = \sum_{k=1}^{N} p_k\left(x,y,z,n\right) \tag{2}$$

where $p_k\left(x,y,z,n\right)$ denotes the acoustic pressure caused by the k-th source acting individually (for $k = 1, 2, \ldots, N$).

2) Acoustic Wave Interference: The phenomenon of interference between acoustic waves is based on the superposition property described above. For formulating this phenomenon, let us assume that there are only two sound sources in the ambient. In this case, Eq. (2) is simplified to

$$p\left(x,y,z,n\right) = p_1\left(x,y,z,n\right) + p_2\left(x,y,z,n\right) \tag{3}$$

which gives the acoustic pressure at any position of three-dimensional space, while the existing acoustic waves interact with each other. The interaction of these two sound waves at a given point (x_0,y_0,z_0) and time index n, is called constructive interference if the absolute value of $p\left(x_0,y_0,z_0,n\right)$ is greater than the absolute values of $p_1\left(x_0,y_0,z_0,n\right)$ and $p_2\left(x_0,y_0,z_0,n\right)$. Otherwise, the interaction is called destructive interference. This definition can be extended for a general case with an arbitrary number of sound sources. The phenomenon of destructive interference is the basis for the creation of a silence zone by ANC devices.

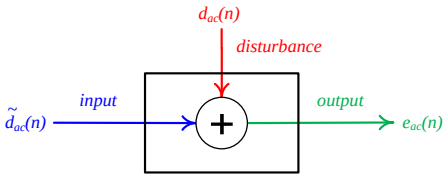

Figure 1. Physical mechanism of active noise control

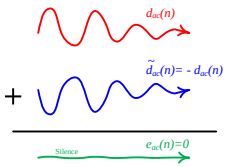

Figure 2. Physical concept of active noise control

II. How to Create a Silence Zone

This section introduces the ANC physical mechanism by which a local silence zone can be created. It is shown that this mechanism should be precisely driven by a digital electronic control system, which can be effectively implemented using a linear digital filter.

A. ANC Physical Mechanism

In single channel ANC, there is a single control source, called the anti-noise source, dealing with an arbitrary number of acoustic noise sources. For this general case, the net acoustic pressure at a given position and time can be mathematically described by using the superposition property as

$$p\left(x,y,z,n\right) = p_d\left(x,y,z,n\right) + p_{\tilde{d}}\left(x,y,z,n\right) \tag{4}$$

where $p_d\left(x,y,z,n\right)$ is the net acoustic pressure at position (x,y,z) and time index n caused by all the existing noise sources, and $p_{\tilde{d}}\left(x,y,z,n\right)$ is the acoustic pressure at the same position and time caused by the anti-noise source acting individually. The unwanted acoustic pressure $p_d\left(x,y,z,n\right)$ itself can be described as the superposition of the acoustic pressures caused by the noise sources acting individually. Now, let us define the following notations.

1) $Z_s\left(x_s,y_s,z_s\right)$ is the position of a desired silence zone in three-dimensional space.
2) $e_{ac}\left(n\right)$ is the net acoustic pressure at Z_s :

$$e_{ac}\left(n\right) \triangleq p\left(x_s,y_s,z_s,n\right) \tag{5}$$

3) $d_{ac}\left(n\right)$ is the acoustic pressure at Z_s caused by all the existing noise sources:

$$d_{ac}\left(n\right) \triangleq p_d\left(x_s,y_s,z_s,n\right) \tag{6}$$

4) $\tilde{d}_{ac}\left(n\right)$ is the acoustic pressure at Z_s caused by the anti-noise (control) source:

$$\widetilde{d}_{ac}\left(n\right) \triangleq p_{\tilde{d}}\left(x_s,y_s,z_s,n\right). \tag{7}$$

Using the above notations, Eq. (4) can be re-expressed as

$$e_{ac}\left(n\right) = d_{ac}\left(n\right) + \widetilde{d}_{ac}\left(n\right), \tag{8}$$

Eq. (8) describes the physical mechanism which is responsible for ANC. The relation between the input and output of this mechanism is shown in Figure 1. According to this figure, the input of this mechanism is the control acoustic pressure at Z_s caused by the anti-noise source, the disturbance signal is the unwanted acoustic pressure at Z_s and the output signal is the net acoustic pressure at Z_s. The ANC physical mechanism generates the output signal as the summation of the input and disturbance signals. From Eq. (8), it can be shown that this output can be made zero if the input and disturbance signals are equal in magnitude and opposite in phase:

$$e_{ac}\left(n\right) = 0 \Rightarrow \widetilde{d}_{ac}\left(n\right) = -d_{ac}\left(n\right). \tag{9}$$

B. Digital Electronic Control System

As discussed above, the ANC physical mechanism can create a silence zone, if the loudspeaker acting as the anti-noise source is precisely driven to produce $\widetilde{d}_{ac}\left(n\right)$ exactly equal to $-d_{ac}\left(n\right)$. For this purpose, the ANC physical mechanism is usually associated with a digital electronic control system which generates a control signal to drive the anti-noise source. This system and its connection to other parts of a general ANC system is illustrated in Figure 3. As can be seen in this figure, one essential component of ANC systems is an error microphone measuring the net acoustic pressure at the desired silence zone. The response of this microphone, hereafter called the error signal, is directly used by the ANC controller as a feedback signal containing information on the performance of the ANC system.

As illustrated in Figure 3, a digital ANC controller generates the control signal $y\left(n\right)$ in response to the input signal $x\left(n\right)$, called the reference signal. In order to generate an effective control signal, the controller requires the reference signal to contain enough information on the unwanted acoustic pressure. In other words, an ideal reference signal is identical to the unwanted acoustic pressure at Z_s; however, this signal can not be measured during the operation of the anti-noise source. This is because $d_{ac}\left(n\right)$ is intended to be combined with the control acoustic pressure generated by the anti-noise source, $\widetilde{d}_{ac}\left(n\right)$. Here, it is useful to continue with an ideal case, where the ideal reference signal, as introduced above, is available:

$$x\left(n\right) = d_{ac}\left(n\right), \tag{10}$$

and where it is assumed that the waveform of the control acoustic pressure at Z_s is exactly equal to that of the control signal used to drive the anti-noise source:

$$\widetilde{d}_{ac}\left(n\right) = y\left(n\right) \tag{11}$$

Now, by substituting Eqs. (10)-(11) into Eq. (9), the desired control signal, denoted by $y_o\left(n\right)$, is obtained as

$$y_o\left(n\right) = -x\left(n\right). \tag{12}$$

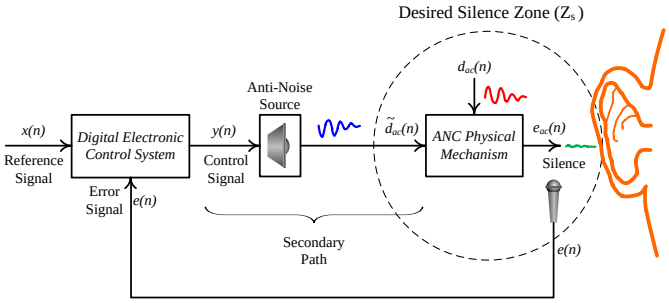

Figure 3. General diagram for ANC

From Eq. (12), the impulse response of the desired ANC controller, $w_o(n)$ is obtained as

$$w_o(n) = -\delta(n) \tag{13}$$

where $\delta(t)$ denotes the Kronecker delta function. In practice, such simple controller can not perfectly create a silence zone at Z_s because of the existence of two constraints, the first of which is $\widetilde{d}_{ac}(n) \neq y(n)$ due to the existence of a physical electro-acoustic channel between the output of the controller and Z_s (usually referred to as the secondary path) and the second of which is $x(n) \neq d_{ac}(n)$ due to the non-measurability of the ideal reference signal. These two constraints and the standard approaches used to deal with are discussed in the following.

C. Secondary Path Constraint

In practice, even if the ANC controller output $y(n)$ is identical to $-d_{ac}(n)$, the control acoustic pressure at Z_s, deviates from $-d_{ac}(n)$. Consequently, the net sound pressure at Z_s deviates from zero. This is because of the existence of an electro-acoustic channel, called the secondary path, between the ANC controller and Z_s. Assuming that $s(n)$ is the impulse response of the secondary path, the control acoustic pressure at Z_s can be expressed as

$$\widetilde{d}_{ac}(n) = s(n) * y(n) \tag{14}$$

where $*$ denotes the convolution operator. Therefore, for producing a control acoustic pressure equal to $\widetilde{d}_{ac}(n)$ at Z_s, the control signal driving the anti-noise source should be set to

$$y(n) = s^{-1}(n) * \widetilde{d}_{ac}(n). \tag{15}$$

From this result, it can be induced that only if the secondary path impulse response is known then the desired control signal $y(n)$ can be estimated.

D. Reference Signal Measurement Constraint

As discussed, an ideal reference signal, which the ANC controller can generate a perfect control signal in response to, is equal to the unwanted acoustic pressure at Z_s. However, this acoustic pressure is not measurable because it is intended to be combined with the control acoustic pressure. Based on the structure upon which ANC devices deal with this constraint, these systems are classified into two major categories: feed forward and feedback.

1) Feed forward Structure*:* This structure for ANC controllers have a long history in digital ANC. This dates back to Widrow's original work on adaptive ANC [6], in which an upstream microphone was used to give information about the unwanted noise propagating down the system. However, most significant reports on feed forward ANC were published in the 1980's, including those published by Morgan [10], Widrow [11], Burgess [12] and Warnaka [13].

Figure 4 shows the diagram of feed forward ANC. As can be seen in this figure, a microphone, called the reference microphone, is located at a far position from Z_s, where the influence of the anti-noise source is not considerable. The response of this microphone is then fed to the controller as the reference signal $x(n)$. However, due to the existence of the distance between the reference microphone and Z_s the waveform of the measured signal $x(n)$ is different to that of $d_{ac}(n)$, which is the ideal reference signal. In the feed forward structure, it is assumed that the ideal reference signal $d_{ac}(n)$ can be modeled as the response of a linear digital filter, called the primary path, to the measured reference signal $x(n)$:

$$d_{ac}(n) = p(n) * x(n), \tag{16}$$

where $p(n)$ is the impulse response of the primary path. Note that the primary path is an hypothetical signal path which is used for modeling the ideal reference signal, unlike the secondary path which is an actual signal path.

2) Feedback Structure*:* As an alternative to the feed forward structure, a feedback structure for ANC controllers was proposed by Eriksson in 1991 [14]. As illustrated in Figure 5, in this structure, $d_{ac}(n)$ is directly estimated by a feedback predictor from the measured error signal $e(n)$. Therefore, since the predicted $d_{ac}(n)$ is directly fed to the ANC controller, there is no signal path between $x(n)$ and $d_{ac}(n)$. In other words, the feedback structure is a special case of the feed forward structure, in which the primary path is simply replaced by an

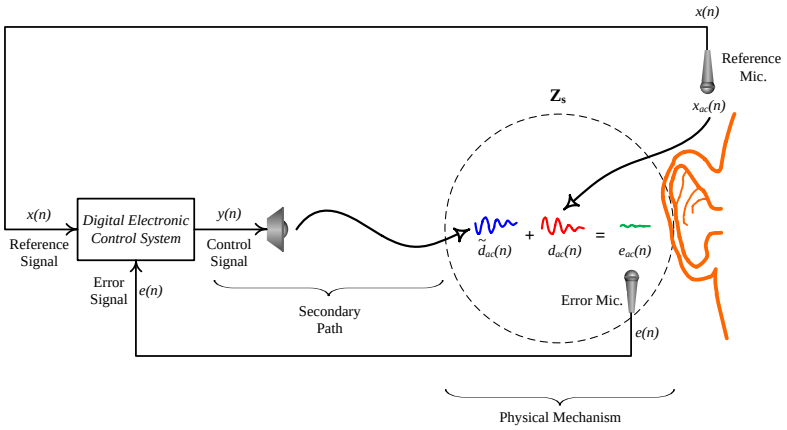

Figure 4. General diagram for feed forward ANC

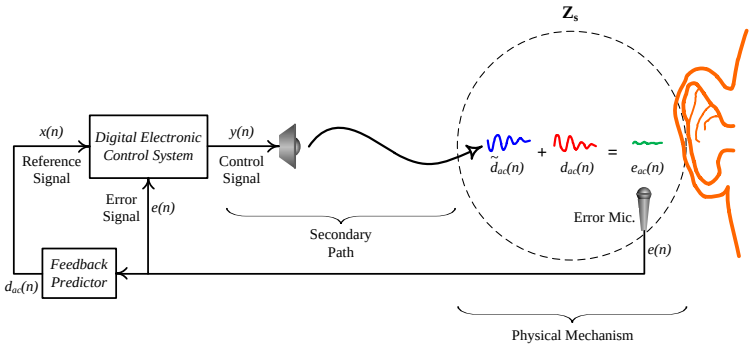

Figure 5. General diagram for feedback ANC

identity system. The main advantage of this structure is that it does not require any reference microphone; therefore, feedback ANC controllers are more compact and cost effective compared to feed forward ANC controllers. However, these controllers can attenuate only the predictable components of the unwanted noise. Furthermore, they are less robust than feed forward ANC controllers. Due to these limitations, successful implementation of these controllers can be found only in specific applications such as personal hearing protection devices [15] and noise canceling headphones [16]–[18].

E. Adjustment of ANC Controller

Considering both the constraints, described above, the net acoustic pressure at the desired silence zone can be expressed by combining Eqs. (14) and (16) as

$$e_{ac}(n) = p(n) * x(n) + s(n) * y(n) \tag{17}$$

Assuming that the error microphone has no effect on the signal waveform (or assuming that this microphone is included in the primary and secondary paths), the response of the error microphone can be approximately expressed as

$$e(n) \approx e_{ac}(n). \tag{18}$$

Now, combining Eqs. (17) and (18) results in

$$e(n) = p(n) * x(n) + s(n) * y(n). \tag{19}$$

Eq. (19) represents a model in terms of electrical signals for the ANC physical mechanism. Considering that $y(n)$ is the response of the ANC controller to $x(n)$, the functional block diagram of this model can be drawn, as shown in Figure 6. From this figure, $e(n)$ can be expressed as

$$e(n) = p(n) * x(n) + \{s(n) * w(n)\} * x(n), \tag{20}$$

where $w(n)$ is the impulse response of the ANC controller. By setting $e(n)$ to zero, the impulse response of the desired ANC controller, $w_o(n)$, can be obtained as

$$w_o(n) = -s^{-1}(n) * p(n) \tag{21}$$

Compared to Eq. (13) which describes an ideal ANC controller, Eq. (21) describes a more realistic ANC controller, considering both the secondary path and reference signal measurement constraints. However, since the impulse responses $p(n)$ and $s(n)$ are usually unknown, the desired ANC controller cannot be directly computed. In this case, the role of Eq. (21) is

reduced to a theoretical proof for the existence of the desired ANC controller.

III. Adaptive Active Noise Control

This section introduces adaptive ANC in which the desired ANC controller can be adaptively adjusted in a system identification framework without having the knowledge of the primary and secondary paths. Also, this section conducts a short review on available algorithms used in adaptive ANC systems.

A. Adaptive Identification of ANC Controller

As a conclusion from the previous section, for realizing the desired ANC controller, it is required to know the impulse responses of the reference and secondary paths, both of which are usually unknown time-varying electro-acoustic channels. To solve this problem, an adaptive scheme for ANC was proposed by Widrow in 1975 [6]. After publishing Widrow's original work, several researchers began to work on this subject [10]–[13]. It was in 1981 that the first successful realization of an adaptive ANC system for acoustic noise propagating in a duct was reported by Burgess [12].

In adaptive ANC, an identification (or adaptation) algorithm continually adjusts the ANC controller w in such a way that an error signal is progressively minimized, rustlings in the gradual convergence of w to w_o. For the realization of such adaptive structure, the digital electronic control system should consist of two distinct parts (Figure 7):

1) A programmable digital filter, w acting as the ANC controller and
2) An adaptation algorithm for the adjustment of the ANC controller.

Usually, the digital filter used as the ANC controller is an standard transversal filter; however, standard adaptation algorithms proposed for the transversal filters e.g. Least Mean Square (LMS) or Recursive Least Square (RLS) can not be used for the automatic adjustment of ANC controllers [8]. A relatively complete but not up-to-date review on adaptation algorithms used in ANC can be found in the book authored by Kuo [7]. A substantial number of other references are listed in this book. Also, the book authored by Elliott [8] provides detailed information on signal processing techniques used in adaptive ANC. In the next section, common ANC adaptation algorithms are briefly reviewed.

B. ANC Algorithms

In ANC systems, standard adaptation algorithm can not be used due to the existence of the secondary path. However, the influence of the secondary path on the performance of any standard adaptation algorithm can be compensated for if the reference signal is filtered using an estimate of the secondary path. This compensation mechanism results in a new range of adaptation algorithms referred to as filtered-x adaptation algorithms. The basic of which is the Filtered-x Least Mean Square (FxLMS) derived by Widrow in 1981 [11].

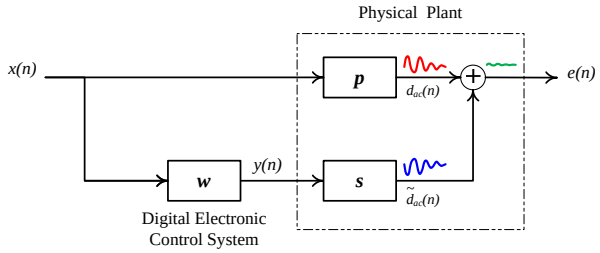

Figure 6. Functional block diagram for general ANC

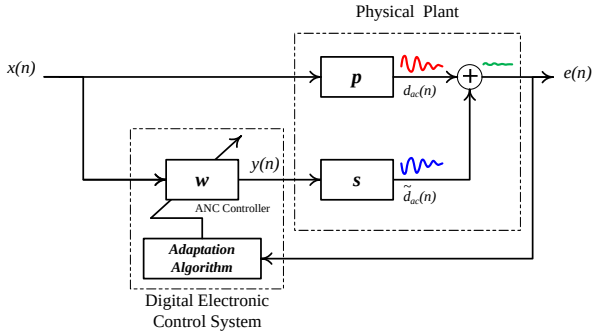

Figure 7. Functional block diagram for adaptive ANC

1) FxLMS Algorithm : FxLMS is a gradient based algorithm which can be used for the identification of an unknown system (e.g. a desired ANC controller) at the presence of a secondary path. The functional block diagram of an FxLMS algorithm adjusting an ANC controller is illustrated in Figure 8. In this figure $\hat{s}$ represents an estimate model of the secondary path. As can be seen, the reference signal is filtered by $\hat{s}$ before being used by the standard LMS algorithm. This is the only difference between the LMS and FxLMS algorithms, resulting the compensation for the secondary path.

2) Variants of FxLMS Algorithm : Other versions of the FxLMS such as Filtered-x Normalized LMS (FxNLMS) [13], Leaky FxLMS [19], Modified FxLMS (MFxLMS) [20] were proposed to improve the performance of the original algorithm. However, the common problem with all of these algorithms is the slow convergence rate, specially when there is a large number of weights (which is usually the case). To overcome this problem, more complicated algorithms such as Filtered-x Recursive Least Square (FxRLS) [21], [22] or Filtered-x Affine Projection (FxAP) [23] can be used. These algorithms have faster convergence rate compared to FxLMS; however they involve matrix computation and their real-time realization is not cost effective.

3) Frequency Domain ANC Algorithms: Above mentioned ANC algorithms suffer from either slow convergence rate or computational complexity. To overcome both of these problems, frequency domain algorithms can be used. The first frequency domain system identification framework was proposed in the 1970's [24] and the first frequency domain ANC

algorithm was developed in 1992 [25]. In this algorithm, the reference and error signals are first stored in buffers to form data blocks. These blocks are then transformed to frequency domain reference and error vectors by a Fast Fourier Transform (FFT). Elements of the frequency domain reference vector is multiplied by filter weights to generate the frequency-domain control vector. Then this vector is fed to an Inverse FFT (IFFT) to produce a block of control signal in time domain. The filter weights, used in the generation of the control signal in frequency domain, are updated by the complex FxLMS algorithm [26]. This algorithm causes a time delay equal to the length of FFT used between the input and output of the ANC controller. This problem would be a shortcoming for the frequency-domain ANC controllers, specially in controlling broad-band stochastic noise.

4) Sub-Band ANC Algorithms: Another approach to overcome both of the computational complexity and slow convergence rate problems associated with ANC algorithms, is based on using the sub-band system identification framework. Conventional sub-band adaptation algorithms introduce a delay into the signal path. This delay cannot be tolerable in ANC systems because these systems are very sensitive to any delay in the secondary path. To overcome this problem, Morgan proposed a delay-less sub-band system identification framework and its FxLMS-based adaptation algorithm in 1995 [27]. Later, Park improved the performance of the Morgan's algorithm [28]. Recently, a number of different algorithms for adaptation of sub-band ANC controllers have been proposed [29]–[31].
In a typical sub-band ANC algorithm, the reference and error signals are divided into sub-bands and then an FxLMS algorithm adjusts a low order transversal filter for each sub-band in order to minimize the corresponding sub-band error signal. In order to avoid the sub-band processing delay, sub-band ANC controllers are not directly used for the generation of the control signals. From weights of sub-band controllers, a full-band transversal ANC controller is constructed. In this scheme, since low order adaptive filters are adjusted in parallel, the convergence rate is fast. Also, since the adaptation process is performed on low order sub-band transversal controllers, the total computational complexity is significantly reduced.

IV. FxLMS-Based ANC Systems

As discussed in the previous section, most ANC algorithms rely on the FxLMS. For this reason, this algorithm is usually known as the basic ANC algorithm. In this section, this algorithm is expressed in ANC framework. Also, main factors limiting the performance of the FxLMS algorithm in ANC systems are discussed.

A. Derivation of FxLMS Algorithm in ANC Framework

As shown in Figure 8, FxLMS-based ANC systems consist of two main components: the ANC controller w, and the FxLMS algorithm, performing an adaptation process on parameters of w. Usually, it is assumed that w is a transversal adaptive filter

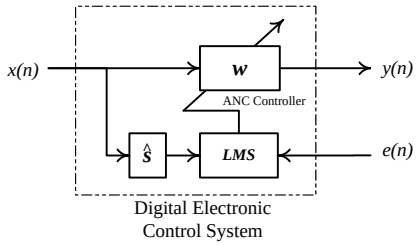

Figure 8. Digital electronic control system in FxLMS-based ANC

of length L. In this case, the control signal $y(n)$, that is the response of w, can be modeled as

$$y(n) = \mathbf{w}^T(n)\,\mathbf{x}(n) \tag{22}$$

where $\mathbf{x}(n)$, called the tap reference vector, is given by

$$\mathbf{x}(n) = \left[\; x(n) \quad x(n-1) \quad \dots \quad x(n-L+1) \;\right]^T \tag{23}$$

and $\mathbf{w}(n)$ is the adaptive weight vector, formed by filter parameters w_0, w_1, ...and w_{L-1} as

$$\mathbf{w}(n) = \left[\; w_0(n) \quad w_1(n) \quad \dots \quad w_{L-1}(n) \;\right]^T \tag{24}$$

The FxLMS algorithm performs an adaptation process on vector $\mathbf{w}(n)$ in such a way that its output, that is $y(n)$, causes the power of the residual acoustic noise $e(n)$ to be minimized. This algorithm is given by

$$\mathbf{w}(n+1) = \mathbf{w}(n) + \mu e(n)\,\mathbf{f}(n) \tag{25}$$

where μ is a scalar parameter, called the adaptation step-size and $\mathbf{f}(n)$ is the filtered reference vector, given by

$$\mathbf{f}(n) = \sum_{q=0}^{Q-1} s_q \mathbf{x}(n-q) \tag{26}$$

In this equation, scalar parameter s_q is the amplitude of the secondary path model impulse response at time index q.

B. Performance of FxLMS Algorithm in ANC

The performance of an FxLMS-based ANC system is limited by a number of related factors that must be addressed in the appropriate order. The absolute maximum level of performance is limited first by the characteristics of the physical plant to be controlled, including the secondary path impulse response and the acoustic noise bandwidth. This means that no matter how good is the electronic control system, the FxLMS will not function properly if the secondary path has a long impulse response and/or the acoustic noise has a wide bandwidth. After the physical plant characteristics, the design parameters of the electronic control system limit the maximum performance achievable. Among these parameters, the most important one is the length of the transversal filter used as the ANC controller. While setting the filter length, it should be considered that although increasing the filter length improves the steady state

performance but it degrades the convergence rate of the process. In addition to this trade-off, the filter length should be set considering the hardware resources available in the electronic control system.

After the filter length is set carefully, the maximum achievable performance is limited by the adaptation step-size μ. In fact, the step-size is the only parameter providing with a control mechanism over the performance of the FxLMS adaptation process. Determining the rules governing on influences of the step-size (μ) on the performance of the FxLMS adaptation process is a complicated subject in adaptive signal processing. However, simplified theoretical analysis, simulation results and even experimental results show that these rules are similar to those derived for the LMS adaptation process. Hence, the rules governing influences of μ on the performance of the LMS adaptation process [32], [33] can be used as rules of thumb for the adjustment of μ in the FxLMS algorithm. These rules can be stated as follows.

1) There is an upper-bound for μ (denoted by μ_{max}) beyond which the process becomes unstable.
2) The convergence rate has a direct relationship with μ and the steady state performance has an indirect relationship with this parameter.

These rules provides a useful sense for setting the step-size; however, there are some ambiguities while using them. For example, the mathematical formulation for μ_{max}, which is available in ANC literature, has been derived only for a pure delay secondary path [7], [8] and the exact value of this bound is unknown for a realistic secondary path.

There have been several contributions, made in the performance analysis of the FxLMS adaptation process in terms of μ. However, only a few have intended to find general closed-form expressions for μ_{max}, steady state performance and convergence speed of this process. Even if such expressions were derived, a simplified cases with pure delay secondary path was considered. This is mainly because of the mathematical complexity associated with the modeling of the FxLMS adaptation process.

Long summarized early work on the analysis of the FxLMS algorithm in [34], [35], while deriving closed-form expressions for μ_{max} and the steady-state performance. However, these expressions were derived only for pure delay secondary paths. In [36], Elliott derived another expression for μ_{max} which was very similar to the one previously derived by Long. The distinction between the two expressions was that Elliott derived his expression specifically for ANC applications. Hence, Elliott's expression for μ_{max} is very popular in ANC literature. In [37], Bjarnason conducted a comprehensive analysis on the FxLMS adaptation process. However, once he intended to derive closed-form expressions for μ_{max} and the steady state performance, he had to simplify his formulations by assuming a pure delay secondary path. Also, Vicente derived another expression for μ_{max} when the acoustic noise is assumed to be sum of deterministic sinusoids [38].

All the aforementioned closed-form expressions for μ_{max} were derived for pure delay secondary paths. However, this assumption is not very realistic because usually a secondary path has a long impulse response. Also, practical results show that the actual value of μ_{max} is different with those have been proposed in available literature so far [39]. Xiao tried to compute μ_{max} for a realistic secondary path but, as he reported in [40], the theoretical results were not in a good agreement with simulation results.

V. Recent Advances in Theoretical Analysis of FxLMS-Based ANC Systems

Recently, the authors have performed a relatively comprehensive theoretical analysis on performance of FxLMS-based ANC systems in realistic conditions. The results, obtained from this study, have been published through several journal and conference papers [41]–[44]. This analysis has been performed based on two different approaches. In the first approach, attention has been focused, foremost, on the derivation of general closed-form expressions for parameters relevant to performance of ANC systems, such as step-size upper-bound, steady state performance and convergence speed of these systems. These expressions has been derived based on a novel stochastic model for ANC systems. In the second approach, attention has been focused on dynamic control of adaptation process performed in ANC systems. For this purpose, the root locus method has been found as a powerful tool for analysis and control of ANC adaptation process dynamics.

A. Closed-from Expression for Step-Size Upper-bound

A relatively comprehensive expression for the upper-bound of the step-size, beyond which FxLMS-based ANC systems become unstable has been derived in [41] as

$$\mu_{max} = \frac{2}{\|\mathbf{s}\|^2 \sigma_x^2 (L + 2D_{eq})} \tag{27}$$

where σ_x^2 is the reference signal power, $\|\mathbf{s}\|$ denotes the norm of the vector formed by the secondary path impulse response coefficients as

$$\mathbf{s} \triangleq \begin{bmatrix} s_0 & s_1 & \dots & s_{Q-1} \end{bmatrix}^T \tag{28}$$

Also, L is the filter length and D_{eq} is a parameter, called the secondary path equivalent delay and computed as

$$D_{eq} \triangleq \frac{\mathbf{s}^T \mathbf{\Psi} \mathbf{s}}{\|\mathbf{s}\|^2} \tag{29}$$

where $\mathbf{\Psi}$ is a diagonal matrix defined as

$$\mathbf{\Psi} = diag\,(0, 1, \dots, Q-1) \tag{30}$$

This expression, given in Eq. (27), is in the form of the commonly-used expression, which was previously derived by Elliott for pure delay secondary paths. However, instead of the physical time delay which appeared in the Elliott's expression, a hypothetical parameter of the secondary path has appeared in our expression. This novel parameter, which is called secondary

path equivalent delay, can be computed for any arbitrary secondary path, unlike the secondary path time delay which is a physical parameter related to only pure delay secondary system.

Also, influences of the acoustic noise band-width on the step-size upper-bound have been investigated in [42]. It has been shown that these influences can be included in the closed-form equation, obtained for the step-size upper-bound as

$$\mu_{max} = \frac{2}{\|\mathbf{s}\|^2 \sigma_x^2 \left(L + \frac{2}{B_w} D_{eq}\right)} \tag{31}$$

where B_w is the normalized bandwidth of the reference signal.

B. Closed-from Expression for Steady State Performance

A closed-form expression for the misadjustment level, determining the relative distance from the actual steady state performance from the optimal performance, has been derived in [41] as

$$\mathcal{M} = \frac{\mu L \|\mathbf{s}\|^2 \sigma_x^2}{2 - \mu \|\mathbf{s}\|^2 \sigma_x^2 (L + 2D_{eq})} \tag{32}$$

Influences of the acoustic noise band-width (B_w) on this expression have been formulated in [42] as

$$\mathcal{M} = \frac{\mu L \|\mathbf{s}\|^2 \sigma_x^2 J_o}{2 - \mu \|\mathbf{s}\|^2 \sigma_x^2 \left(L + \frac{2}{B_w} D_{eq}\right)} \tag{33}$$

Based on the above expressions for $\mathcal{M}$, the steady state residual noise power can be obtained as

$$\sigma_x^2 = (1 + \mathcal{M}) J_o \tag{34}$$

where J_o is the optimal MSE function, which can be interpreted as the minimum achievable residual noise power.

VI. Computer Simulation

In this section, the validity of the theoretical expressions given in Section V is demonstrated using computer simulation and numerical analysis.

A. Upper-Bound of Step-Size

The existence of an upper-bound for the adaptation step-size, beyond which the system becomes unstable, can be also shown by using computer simulation. For this purpose, different simulation experiments with different step-sizes should be conducted. For example, plots of Figure 9 show variations of the MSE function (mean square of error signal) in three simulation experiments with different values of μ. As can be seen, when μ is set to 0.02 or 0.08, the system becomes stable. However, when it is set to 0.12, the system becomes unstable. Therefore, it can be seen that the upper-bound for the step-size locates between 0.08 and 0.12.

In order to find a more accurate upper-bound more simulation experiments should be conducted. The value of the step-size should be changed incrementally (with the incremental step of 0.001) until the system becomes unstable. For each particular value of the step-size, 100 independent simulation runs are repeated. Therefore, for each step-size, the number of stable experiments can be interpreted as the percentage of the stable experiments. According to the results obtained, for step-sizes below 0.089, all the simulation experiments are stable ($\mu_D = 0.089$). When the step-size is increased to 0.090, only 68% of experiments become stable. Also, for step-sizes beyond 0.099, there is no stable experiment ($\mu_U = 0.09$). Therefore, μ_D can be considered as the maximum step-size below which the stability of the system can be assured. Similarly, μ_U can be considered as the minimum step-size beyond which the system can never become stable. Therefore, the actual upper-bound for the step-size locates between these two bonds. Herein, it is assumed that the upper-bound is in the middle of μ_D and μ_U:

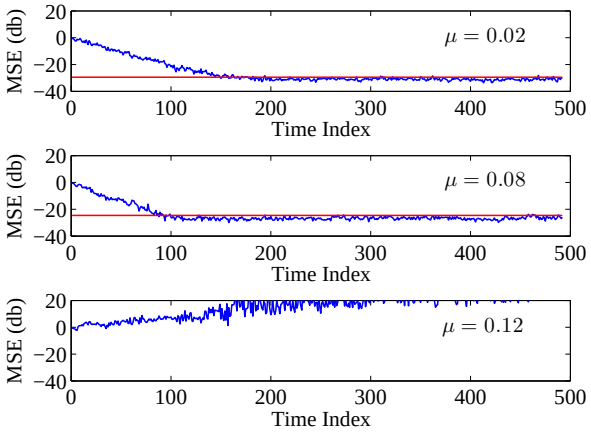

Figure 9. Variations of MSE function for different values of step-size

$$\mu_{max} \approx \frac{\mu_D + \mu_U}{2} \tag{35}$$

Therefore, from the simulation results described above, it can be shown that

$$\mu_{max} \approx 0.0945, \qquad in\ simulation \tag{36}$$

On the other hand, from Eq. (27), a theoretical value for μ_{max} can be obtained. For the secondary path impulse response, used in the simulation, the theoretical upper-bound for the adaptation step-size can be computed as

$$\mu_{max} = 0.0951, \qquad in\ theory \tag{37}$$

Comparing values of μ_{max}, obtained from computer simulation and the the proposed theoretical expression, given in Eq. (27), confirms the validity and accuracy of Eq. (27) .

In order to determine the influence of the acoustic noise bandwidth on the step-size upper-bound of the simulated system, the simulation experiment, described above, are repeated for different band-limited acoustic noise. In simulation with each noise bandwidth, an actual value for the upper-bound of the step-size can be obtained, as described above. The results

are plotted in Figure 10. Also, the theoretical results, obtained by plotting Eq. (31) with respect to the bandwidth B_w, is shown in this figure by solid red line. The agreement between the actual upper-bound, obtained from simulation results and the theoretical one, obtained from Eq. (31), is evident.

B. Steady-State Residual Acoustic Noise Power

Eqs. (32) and (34) give a closed-form expression for the steady-state residual noise power parameter, considering a general secondary path. Simulation results show that these expressions can precisely determine the steady-state performance of FxLMS-based ANC systems. For example, in plots of Figure 9, red lines show the steady-state level of each MSE function, obtained by using this equation. As can be seen, for all of the three cases, the theoretical result can be precisely matched to the simulation result. Note that, for computing the steady-state level, it is required to compute constant J_o. This parameter can be computed by using the reference signal statistics as shown in [41].

In order to show the general validity of Eq. (33), more simulation runs with different values for the step-size are conducted. The results are then plotted in Figure 11. In this figure, the red curve is obtained by plotting Eq. (34) in with respect to the adaptation step-size (μ). Also, the blue curve is plotted by using simulation results. As can be seen, for the allowed range of the adaptation step-size, theoretical and simulation results are in a good agreement.

In order to investigate the influence of the acoustic noise band-width on the steady state performance, the simulation experiment, discussed above, can be repeated for different band-limited acoustic noise signals. Figure 12 shows variations of the steady-state residual acoustic noise power with respect to the adaptation step-size for band-limited acoustic noise with $B_w = 0.8$. As can be seen, Eq. (33) can precisely consider the influence of the acoustic noise bandwidth on the steady-state residual acoustic noise power. Results obtained from simulation experiments with different values for B_w leads to the same conclusion; however, these results are not mentioned here for the available limit of space.

VII. Conclusion

This paper conducted a short review on FxLMS-based ANC systems. After describing the physical idea behind ANC, different structures which can be used in the realization of ANC system have been introduced. It is argued that the FxLMS algorithm is a fundamental adaptation algorithm in ANC. The theoretical work on analysis of FxLMS-based ANC systems has usually considered simplified cases in order to avoid mathematical difficulties. However, these conditions are not realistic. Recent advances in theoretical analysis of FxLMS algorithm have solved this problem. Theoretical findings for general case with a general secondary path and a general band-limited acoustic noise have been represented. Simulation results showed the validity of these theoretical findings.

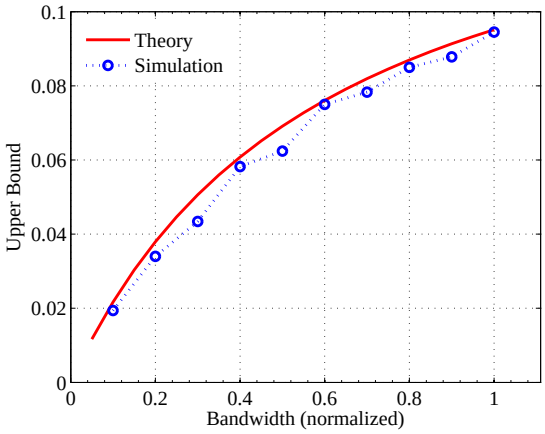

Figure 10. Verification of the theoretical expression for formulating the influence of acoustic noise bandwidth on μ_{max}

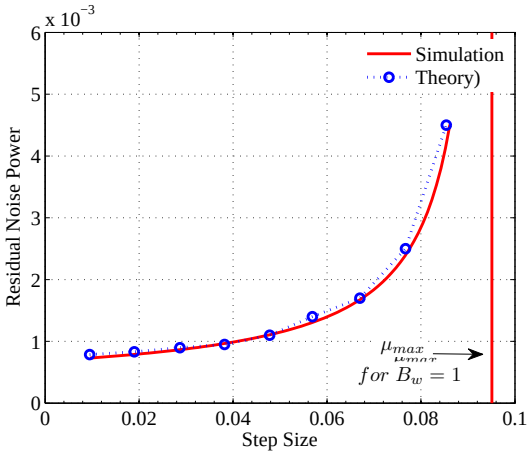

Figure 11. Verification of the proposed theoretical expression for steady-state acoustic noise power

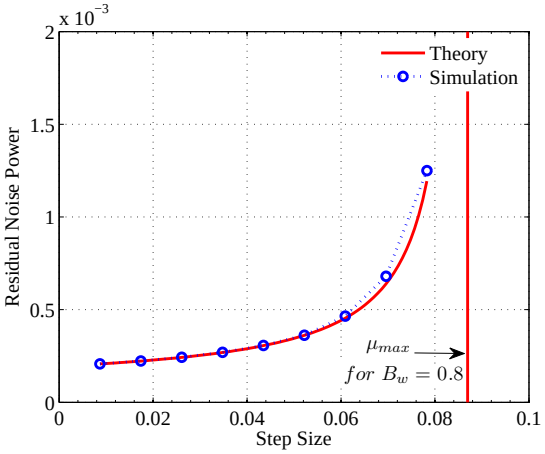

Figure 12. Verification of the proposed theoretical expression for formulating the influence of acoustic noise bandwidth on the steady-state performance

REFERENCES

[1] P. Leug, "Process of silencing sound oscillations," *U.S. Patent 2043416*, 1936.

[2] H. F. Olson and E. G. May, "Electronic sound absorber," *Journal of the Acoustical Society of America*, vol. 25, no. 4, pp. 829–829, 1953.

[3] H. F. Olson, "Electronic control of noise, vibration and reverberation," *Journal of the Acoustical Society of America*, vol. 28, pp. 966–972, 1956.

[4] L. G. Fogel, "Methods of improving intelligence under random noise interference," *U.S. Patent 2866848*, 1958.

[5] E. D. Simshauser and M. E. Hawley, "The noise canceling headset - an active ear defender," *Journal of the Acoustical Society of America*, vol. 27, pp. 207–217, 1955.

[6] B. Widrow, J. Glover, J. McCool, J. Kaunitz, C. Williams, R. Hearn, J. Zeidler, J. Eugene Dong, and R. Goodlin, "Adaptive noise cancelling: principles and applications," *Proceedings of the IEEE*, vol. 63, no. 12, pp. 1692–1716, December 1975.

[7] S. M. Kuo and D. R. Morgan, *Active noise control systems: algorithms and DSP implementations*. New York, NY, USA: Wiley Interscience, 1996.

[8] S. J. Elliott, *Signal Processing for Active Control*. San Diego, CA.: Academic Press, 2001.

[9] D. Reynolds, *Engineering Principles of Acoustics: Noise and Vibration Control*. Boston, USA: Allyn and Bacon Inc., 1981.

[10] D. R. Morgan, "An analysis of multiple correlation cancellation loops with a filter in the auxiliary path," *Acoustics, Speech, and Signal Processing, IEEE International Conference on ICASSP '80.*, pp. 457–461, April 1980.

[11] B. Widrow, D. Shur, and S. Shaffer, "On adaptive inverse control," in *Proceeding of the 15th Asilomar Conference on Circuits, Systems and Computers*, November 1981, pp. 185–189.

[12] J. C. Burgess, "Active adaptive sound control in a duct: computer simulation," *Journal of the Acoustical Society of America*, vol. 70, pp. 715–726, 1981.

[13] G. E. Warnaka, L. A. Poole, and J. Tichy, "Active acoustic attenuators," *U.S. Patent 4473906*, 1984.

[14] L. J. Eriksson, "Recursive algorithms for active noise control," *International Symposium of Active Control of Sound and Vibration*, pp. 137–146, 1991.

[15] B. Rafaely and S. Elliott, "H_2/H_∞ active control of sound in a headrest: design and implementation," *Control Systems Technology, IEEE Transactions on*, vol. 7, no. 1, pp. 79 –84, jan. 1999.

[16] T. Meurers, S. Veres, and S. Elliot, "Frequency selective feedback for active noise control," *Control Systems Magazine, IEEE*, vol. 22, no. 4, pp. 32 – 41, aug. 2002.

[17] Y. Song, Y. Gong, and S. Kuo, "A robust hybrid feedback active noise cancellation headset," *Speech and Audio Processing, IEEE Transactions on*, vol. 13, no. 4, pp. 607–617, July 2005.

[18] I. Tabatabaei Ardekani and W. H. Abdulla, "Allpass filtered reference LMS algorithm for adaptive feedback active noise control," *Proceeding of 2009 Asia Pacific Signal and Information Processing Association Annual (APSIPA) Summit and Conference, Sapporo, Japan*, pp. 859–865, 2009.

[19] S. Elliott, I. M. Stothers, and P. A. Neslson, "A multiple error LMS algorithm and its applications to active control of sound and vibration," *Acoustic, Speech and Signal Processing Processing, IEEE Transactions on*, vol. 35, pp. 1423–1434, 1987.

[20] M. Rupp and A. Sayed, "Two variants of the fxlms algorithm," pp. 123 –126, oct 1995.

[21] A. Oppenheim, E. Weinstein, K. Zangi, M. Feder, and D. Gauger, "Single-sensor active noise cancellation," *Speech and Audio Processing, IEEE Transactions on*, vol. 2, no. 2, pp. 285 –290, apr. 1994.

[22] L. Eriksson, M. Allie, D. Melton, S. Popovich, and T. Laak, "Fully adaptive generalized recursive control system for active acoustic attenuation," *Acoustics, Speech, and Signal Processing, 1994. ICASSP-94., 1994 IEEE International Conference on*, vol. ii, pp. II/253 –II/256 vol.2, apr. 1994.

[23] A. Gonzalez, M. Ferrer, M. de Diego, and G. Pinero, "Fast filtered-x affine projection algorithm for active noise control," pp. 162 – 165, oct. 2005.

[24] T. Walzman and M. Schwartz, "Automatic equalization using the discrete frequency domain," *Information Theory, IEEE Transactions on*, vol. 19, no. 1, pp. 59 – 68, jan. 1973.

[25] Q. Shen and A. Spanias, "Time and frequency domain x-block lms algorithms for single channel active noise control," in *International Congress on Recent Developments in Air- and Structure-Borne Sound andVibration*, 1992, pp. 353–360.

[26] K. M. Reichard and D. C. Swanson., "Frequency domain implementation of the filtered-x algorithm with online system identification," *Proc. Recent Advances in Active Sound Vibration*, pp. 562–573, 1993.

[27] D. Morgan and J. Thi, "A delayless subband adaptive filter architecture," *Signal Processing, IEEE Transactions on*, vol. 43, no. 8, pp. 1819–1830, Aug 1995.

[28] S. J. Park, J. H. Yun, Y. C. Park, and D. H. Youn, "A delayless subband active noise control system for wideband noise control," *Speech and Audio Processing, IEEE Transactions on*, vol. 9, no. 8, pp. 892–899, Nov 2001.

[29] B. Siravara, N. Magotra, and P. Loizou, "A novel approach for single microphone active noise cancellation," *Circuits and Systems, 2002. MWSCAS-2002. The 2002 45th Midwest Symposium on*, vol. 3, pp. III–469–III–472 vol.3, Aug. 2002.

[30] V. DeBrunner, L. DeBrunner, and L. Wang, "Sub-band adaptive filtering with delay compensation for active control," *Signal Processing, IEEE Transactions on*, vol. 52, no. 10, pp. 2932–2941, Oct. 2004.

[31] I. Tabatabaei Ardekani and W. H. Abdulla, "A new subband algorithm for active attenuation of broadband noise," *Proceeding of 2009 International Symposium on Active Control of Sound and Vibration (ACTIVE), Ottawa, Canada*, August 2009.

[32] B. Widrow, J. McCool, M. Larimore, and J. Johnson, C.R., "Stationary and nonstationary learning characteristics of the lms adaptive filter," *IEEE Proceedings*, vol. 64, no. 8, pp. 1151–1162, Aug. 1976.

[33] H. Butterweck, "A wave theory of long adaptive filters," *Circuits and Systems I: Fundamental Theory and Applications, IEEE Transactions on*, vol. 48, no. 6, pp. 739–747, Jun 2001.

[34] G. Long, F. Ling, and J. Proakis, "The LMS algorithm with delayed coefficient adaptation," *Acoustics, Speech and Signal Processing, IEEE Transactions on*, vol. 37, no. 9, pp. 1397–1405, September 1989.

[35] ——, "Corrections to 'The LMS algorithm with delayed coefficient adaptation'," *Signal Processing, IEEE Transactions on*, vol. 40, no. 1, pp. 230–232, January 1992.

[36] S. J. Elliott and P. A. Nelson, "Multiple-point equalization in a room using adaptive digital filters," *Journal of the Audio Engineering Society*, vol. 37, no. 11, pp. 899–907, November 1989.

[37] E. Bjarnason, "Analysis of the filtered-x LMS algorithm," *Speech and Audio Processing, IEEE Transactions on*, vol. 3, no. 6, pp. 504–514, November 1995.

[38] L. Vicente and Masgrau, "Novel FxLMS Convergence Condition With Deterministic Reference," *Signal Processing, IEEE Transactions on*, vol. 54, no. 10, pp. 3768–3774, October 2006.

[39] Y. Takenouchi, H. Sizuhi, and A. Omoto, "Behavior of the practically implemented filtered reference LMS algorithm in an active noise control system," *Journal of Acoustical science and technology*, vol. 27, pp. 20–27, 2006.

[40] Y. Xiao, A. Ikuta, L. Ma, and K. Khorasani, "Stochastic Analysis of the FXLMS-Based Narrowband Active Noise Control System," *Audio, Speech, and Language Processing, IEEE Transactions on*, vol. 16, no. 5, pp. 1000–1014, July 2008.

[41] I. Tabatabaei Ardekani and W.H. Abdulla, "Theoretical convergence analysis of FxLMS algorithm," *Signal Processing*, vol. 90, no. 12, pp. 3046 – 3055, 2010.

[42] ——, "On the convergence of real-time active noise control systems," *Signal Processing*, vol. 91, no. 5, pp. 1262 – 1274, 2011.

[43] ——, "On the stability of adaptation process in active noise control systems," *Journal of Acoustical Society of America*, vol. 129, no. 1, pp. 173–184, 2011.

[44] I. T. Ardekani and W. Abdulla, "Study of convergence behaviour of real-time adaptive active noise control systems," in *Proceedings of 2010 Asia Pacific Signal and Information Processing Association Annual (APSIPA) Summit and Conference, Biopolis, Singapore, 14-17 December 2010, Pages 534-537.*